Reducing Hurricane-induced Power Outages through Preventive Operation

Yuanrui Sang, *Student Member, IEEE*, Jiayue Xue, Mostafa Sahraei-Ardakani, *Member, IEEE*, Ge Ou, *Member, IEEE*

***Abstract*—Severe weather is the primary cause of power outages in the U.S. Despite the availability of weather forecast information to power system operators, such data is not systematically integrated in operation models. This paper is the first to develop an integrated platform to convert the weather data into appropriate information for operation, during hurricanes. To do so, first, a structural model of the transmission towers is developed to enable stability analysis with dynamic wind loading. The model produces failure probabilities as a function of the wind speed. These probabilities are, then, integrated within a day-ahead security-constrained unit commitment framework to guide preventive operation. The resulting day-ahead schedule will be more secure as it will rely less on the elements that are likely to fail due to the hurricane. Simulation studies are conducted on IEEE 118-bus system, affected by synthesized Irma and Harvey hurricanes, to test the effectiveness of the method. The platform, presented in this paper, was able to prevent 33% to 83% of the blackouts induced by the hurricanes, in our simulation studies. Further research is required to investigate the impacts of flooding, damage to the distribution network, and the influence of weather forecast uncertainty.**

***Index Terms*—Dynamic structural modeling, extreme events, hurricane, power outage, power system reliability, preventive operation, stochastic optimization, transmission outage.**

I. Nomenclature

A. Structural Model

Indices

l	Coefficient compared with limit state.
k	Transmission line.
i, j	Location indices of the transmission tower.
nt	Dimension of the wind loadings on one transmission tower.
m	Indices of tower locations in the transmission line.

Variables

$F_R(V)$	Structural wind fragility at wind speed V.
$F_d(t)$	Wind load at time t.
ω	Fluctuating wind circular frequency.
$H(\omega)$	Decomposed matrix of cross spectral density matrix by Cholesky decomposition.
$S(\omega)$	Cross spectral density matrix.
f	Fluctuating wind frequency.
$S_i(z_i, f)$	Auto power spectrum at height z_i at frequency f.
$S_{ij}(r, f)$	Cross spectral density spectrum of node i and j at a distance of r at frequency f.
$S_{jj}(z_j, f)$	Auto power spectrum at height z_j at frequency f.
$S_v(f)$	Auto power spectrum of fluctuating wind at frequency f.
$v_j(t)$	Fluctuating wind speed on node j at time t.
$v_j(y_j, z_j, t)$	Fluctuating wind speed at transverse coordinate y_j at height z_j at time t.
V	Mean wind speed.
$V(t)$	Wind time history.
$V_g(r_g)$	Gradient wind speed at a radial distance of r_g from hurricane center.
$\bar{V}(z_i)$	Mean wind speed at height z_i.
$\theta_{jm}(\omega_{ml})$	Compound angle of $H_{jm}(\omega_{ml})$.
r_g	Radial distance from hurricane center.
$F_R(V)$	Tower failure probability under wind speed V.
V_m	Mean wind speed at the m^{th} tower location.
P_m	Damage and failure probability.
$P[FL, k]$	Failure probability of transmission line k.
$P[SL, k]$	Survival probability of transmission line k.

Parameters

A, B	Scaling parameters for horizontal wind profile calculation.
A_P	Projected area.
C_d	Drag coefficient.
C_y	Horizontal related exponential coefficient.
C_Z	Vertical related exponential coefficient.
f_c	Coriolis parameter.
K_T	Stiffness matrix of lumped mass model.
LS	Limit state of structure.
N	Positive large integer.
p_n	Ambient pressure.
p_c	Central pressure.
V_{10}	Mean wind speed at height10m.
$\bar{V}$	Mean wind speed.
$\bar{V}_{10}$	10-minute mean wind speed at the height of 10m.
y_i	Transverse coordinate at node i.
y_j	Transverse coordinate at node j.
z	Height of mean wind speed.
z_{10}	Height constant of 10m.
α	Ground roughness.
ρ	Air density.
φ_{ml}	Independent uniform distribution phase angle.
ω_{up}	Cut-off frequency.
$\Delta\omega$	Frequency increment.
NT	Number of towers in one transmission line.

B. Preventive Operation Model

Indices

Y. Sang and M. Sahraei-Ardakani are with the Electrical and Computer Engineering Department, University of Utah. J. Xue and G. Ou are with the Civil Engineering Department, University of Utah, Salt Lake City, UT 84112 USA (e-mail: {yuanrui.sang; jiayue.xue; ge.ou; mostafa.ardakani}@utah.edu).

k Transmission line.
g Generator.
n Node.
s Scenario.
seg Segment of linearized generator cost function.

Sets
$\sigma^+(n)$ Transmission lines with their "to" bus connected to node n.
$\sigma^-(n)$ Transmission lines with their "from" bus connected to node n.
$g(n)$ Generators connected to node n.

Variables
$F_{k,s,t}$ Real power flow through transmission line $k$in scenarios s at time t.
$L^L_{n,s,t}$ Load loss at node $n$in scenarios at time t.
$P_{g,s,t}$ Real power generation of generator g in scenarios at time t.
$P^O_{g,s,t}$ Over-generation of generator g in scenarios at time t.
$P^{seg}_{g,s,t}$ Real power generation of generator g in scenarios in segment seg at time t.
$u_{g,t}$ Unit commitment (1: generator g is on at time t; 0: generator g is off at time t.)
$v_{g,t}$ Startup variable (1: generator g starts up at time t; 0: generator g does not start up at time t.)
$w_{g,t}$ Shutdown variable (1: generator g shuts down at time t; 0: generator g does not shut down at time t.)
$\theta_{n,s,t}$ Voltage angle at bus n in scenarios at time t.
$\theta_{fr,k,s,t}$ Voltage angle at the "from" node of line k in scenarios at time t.
$\theta_{to,k,s,t}$ Voltage angle at the "to" node of line $k$in scenarios at time t.

Parameters
b_k Susceptance of transmission line k.
$c^{linear}_{g,seg}$ Linear cost of generator g in segment seg.
c^L Cost of load loss ($/MWh).
c^{NL}_g No load cost of generator g.
c^O Cost of over generation ($/MWh).
c^{SD}_g Shutdown cost of generator g.
c^{SU}_g Startup cost of generator g.
F^{max}_k Thermal/stability limit of transmission line k.
$L_{n,s,t}$ Load at bus $n$in scenario s at time t.
N_b Number of buses in s system.
N_g Total number of generators.
N_s Number of scenarios.
N_{seg} Number of segments for the linearized generator cost function.
p_{k,t_k} Probability of line k to fail at time t_k.
p_s Probability of scenario s.
P^{max}_g Upper generation limit of generator g.
P^{min}_g Lower generation limit of generator g.
$P^{seg,max}_g$ Upper generation limit of generator g in segment seg.
RR_g Hourly ramp-rate for generator g.
t_H The time that hurricane starts.
t_k The time that line k fails.
T Length of the investigated time period.
T_F Number of time periods with different probabilities of transmission line failure.
T^{down}_g Minimum down time for generator g.
T^{up}_g Minimum up time for generator g.
$z_{k,s,t}$ Transmission line k's status at time t in scenario s (1: line is closed; 0: line is open).
$\Delta\theta^{max}_k$ Maximum value of bus voltage angle difference to maintain stability for line k.
$\Delta\theta^{min}_k$ Minimum value of bus voltage angle difference to maintain stability for line k.

II. Introduction

According to a report by the Department of Energy, severe weather is the leading cause of power outages in the U.S. [1]. Hurricanes and tropical storms are one main category of extreme weather events that lead to large blackouts, both in terms of lost electric load and number of affected customers[2], [3]. The 2017 hurricane season clearly revealed the vulnerability of the U.S. electric power grid to the hurricanes. In August 2017, hurricane Harvey caused about 300,000 customer outages in Texas [4]. About two weeks later, in September, hurricane Irma led to outage of more than 6 million customers in Florida (59% of total FL customers) [5] and just below a million customers in Georgia (22% of total GA customers) [6]. Later in September, hurricane Maria made a devastating landfall in Puerto Rico, which left the entire island in complete darkness [7]. As of the end of 2017, more than three months after the hurricane's landfall, still about 30% of the load was not recovered. Clearly, the existing reliability practices are inadequate under hurricanes.

Power system reliability is often achieved through implementation of various redundancies, so that the system withstands likely disturbances [8]–[10]. Reliability standards set by North American Electric Reliability Corporation (NERC) require the operators to prevent blackouts under the random outage of one (*N*-1) or two (*N*-1-1) bulk power elements [11], [12]. Hurricanes, however, usually lead to outage of multiple elements, well beyond the conditions of NERC standards. For example, Electric Reliability Council of Texas (ERCOT) experienced 97 transmission line outages (139 kV and above) after hurricane Harvey made landfall [13]; similarly, hurricane Sandy caused the outage of over 218 high-voltage (115 kV and above) transmission lines [14]. Clearly, the conventional reliability tools, which the industry makes use of, are neither designed for, nor applicable to such extreme conditions.

For the case of hurricanes, rich meteorological information, such as wind direction and speed, is forecasted and available to power system operators [14], [15]. Some system operators even have access to meteorologists onsite [14]. However, the weather information is often not converted to appropriate inputs for systematic use in preventive operation. The conservative changes to the operation procedures, during severe weather, is heavily based on engineering judgement and operators' knowledge. Thus, many effective but unknown preventive actions are missed, increasing the size of power outages.

There is a vast body of literature which aims to estimate the power outage statistics (e.g., number of customers without power, etc.) with the weather forecast data before the hurricane [16]–[23]. Such statistical models, though may produce high-

quality results, are only able to provide macro-scale statistics about the outage, without any details on the element-level failures. There also exists a number of studies on optimizing the repair and restoration plan after the hurricane [24]–[27]. However, the literature on preventive operation during the hurricane, using weather forecast information, is almost nonexistent. The only published research in this domain that we are aware of includes [28] and the authors' own study [29]. Both [28] and [29] show promising prospect for preventive operation; however, they do not properly model the weather data, estimate the damage to power system component through dynamic structural analysis, and integrate the predicted damage information in day-ahead operation. This paper is the first to develop such an integrated framework and analyze the effectiveness of preventive day-ahead operation under synthesized hurricanes. In reality, the weather forecast information includes inherent uncertainties [30]; however, this paper primarily focuses on exploring the feasibility and effectiveness of preventive operation assuming that the weather forecast is exact.

It is important to acknowledge that this paper exclusively focuses on the transmission-level component damages. Historic data verifies that generators are usually not prone to damage by hurricanes, as they are protected in an indoor environment with strong structural support [31]; a small number of issues are reported for generators due to flooding. The same report confirms that hurricanes cause significant damage to distribution and transmission systems [31]. Due to the radial arrangement of the distribution network, there is very little room for preventive operation at the distribution level. We acknowledge the vulnerability of the distribution network to severe weather, but we overlook that in this paper. To further justify this assumption, it is important to note that power outages caused by distribution-level damages are local. However, transmission-level failures could lead to power outages far outside the area directly affected by the hurricane, with healthy distribution networks. Such outages are likely avoidable through advanced models that enable employment of weather forecast data in preventive operation. This is precisely what the current paper intends to achieve. In doing so, this paper also exclusively focuses on the wind feature of the hurricanes, ignoring other factors like flooding. Again, we acknowledge that flooding may damage the power system components. However, the majority of the failures during a hurricane is caused by its strong winds.

This paper, first, employs weather forecast information, which mainly includes wind speed, to estimate the damages to transmission system components. To do so, a structural model is developed, which analyzes the failure of transmission towers, due to the dynamic wind loading. The model estimates the likelihood of transmission line failure as a function of wind speed.

The estimated failure probabilities are then explicitly modeled within the day-ahead security-constrained unit commitment (SCUC). Load shedding, in the SCUC formulation, is penalized at a high cost. Thus, electric load will only be shed if the damaged network cannot support the delivery of energy to that location, or if such delivery is extremely costly. The mathematical representation of this problem is a stochastic mixed-integer linear program. To reduce the computational burden of the problem, a simple scenario reduction technique is used. The schedule, calculated through this framework, will rely less on the transmission elements that are prone to failure due to the hurricane. Thus, the system reliability will be enhanced and the power outage will be reduced.

The simulation results, presented in this paper, suggest that appropriate integration of weather data in power system operation will significantly reduce power outages during a hurricane event. This reduction in our simulation studies, for IEEE 118-bus system under synthesized Irma and Harvey hurricane scenarios were anywhere between 33% and 83%, which is rather encouraging.

The rest of this paper is organized as follows. Section III presents the transmission tower structural model and its stability under dynamic wind loading. Section IV describes generation of contingency scenarios, using the failure probabilities, estimated through the structural model. Section V develops the preventive SCUC model using stochastic optimization. Case studies are presented and discussed in Section VI. A brief discussion of the computational complexity of the model is presented in Section VII and finally, section VIII concludes this paper.

III. Transmission Tower Dynamic Response under Wind Loading

This section briefly explains the derivation of a finite element model of transmission towers to enable fragility analysis. All the towers are assumed to follow a generic design [32], with the height of 55 m, steel-made members (ASTM A-36), and L-shaped cross sections. A finite element model of this tower is built in ANSYS. To reduce the computational time, the tower model is further reduced into a 13 degree of freedom lumped massed model as shown in Fig. 1. Stiffness matrix K_T of the lumped mass model of 13 degrees of freedom is derived from the finite element model through flexibility method [33].

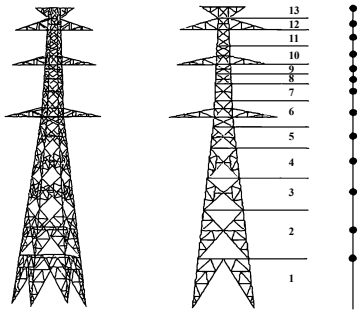

Fig. 1. Finite element model and simplified model of transmission towers.

Dynamic wind loading characteristics are composed with steady and fluctuating wind components [34]. For mean wind component, the changes over height is described by the power law [35] as shown in (1). As most transmission towers are built in the open plain, α equals 0.16.

$$\frac{\bar{V}}{\bar{V}_{10}} = \left(\frac{z}{z_{10}}\right)^{\alpha} \tag{1}$$

Fluctuating wind speed is simulated through WAWS method. According to the wind speed record, fluctuating wind speed can be expressed as a Gaussian stationary random process [36]. The cross spectral density matrix for an *nt*-dimensional zero-mean stationary Gaussian random process $v_j(\mathrm{t})(\mathrm{j} = 1,2,\cdots,\mathrm{nt})$ is presented in (2).

$$S(\omega) = \begin{bmatrix} S_{11}(\omega)S_{12}(\omega)\cdots S_{1n}(\omega) \\ S_{21}(\omega)S_{22}(\omega)\cdots S_{2n}(\omega) \\ \cdots \\ S_{nt1}(\omega)S_{nt2}(\omega)\cdots S_{ntnt}(\omega) \end{bmatrix} \tag{2}$$

In order to obtain the power spectrum of fluctuating wind, Davenport spectrum [37] is used. The auto power spectrum of fluctuating wind is calculated in (3).

$$S_v(f) = 4\alpha\overline{V_{10}}^{-2}\frac{x^2}{f(1+x^2)^{4/3}} \quad x = \frac{1200f}{\overline{V_{10}}} \tag{3}$$

Based on the auto power spectrum of 13 nodes, the cross spectral density spectrum can be calculated as shown in (4)-(5).

$$S_{ij}(r,f) = \sqrt{S_{ii}(z_i,f)S_{jj}(z_j,f)}Coh(r,f)\ i \neq j \tag{4}$$

$$Coh(r,f) = exp\left(\frac{-2f\sqrt{C_y^2(y_i-y_j)^2+C_z^2(z_i-z_j)^2}}{\overline{V}(z_i)+\overline{V}(z_j)}\right) \tag{5}$$

In this research, we choose $C_y = 8$ and $C_Z = 7$. Therefore, the cross spectral density matrix can be obtained, and decomposed, using Cholesky decomposition, as shown in (6)-(7).

$$S(\omega) = H(\omega)H^*(\omega)^T \tag{6}$$

$$H(\omega) = \begin{bmatrix} H_{11}(\omega) & 0 & \cdots & 0 \\ H_{21}(\omega)H_{22}(\omega) & & \cdots & 0 \\ \cdots\cdots\cdots & & & \\ H_{nt1}(\omega)H_{nt2}(\omega)\cdot & \cdot\cdot & H_{ntnt}(\omega) & \end{bmatrix} \tag{7}$$

According to Shinozuka theory, the fluctuating wind can be represented by (8)-(9) [38].

$$v_j(y_j,z_j,t) = \sqrt{2(\Delta\omega)}\sum_{m=1}^{j}\sum_{l=1}^{N}\left|H_{jm}(\omega_{ml})\right| cos(\omega_{ml}t - \theta_{jm}(\omega_{ml}) + \varphi_{ml}) \quad j = 1,2,\cdots,\ nt \tag{8}$$

$$\omega_l = (l-1)\Delta\omega + \frac{m}{N}\Delta\omega, l = 1,2,\cdots,\ N \tag{9}$$

Fluctuating wind component is simulated using the above equations. There are 13 wind speed at different heights based on the division of the transmission tower. The top tower fluctuating wind time history is shown in Fig. 2-top; the fluctuating wind speed is further compared with the desired power spectrum, as shown in Fig. 2-bottom.

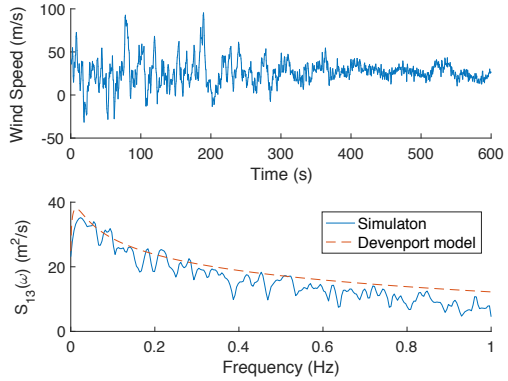

Fig. 2. Wind time history and validation; top: wind speed at the tower tip; bottom: comparison between simulated and theoretical value.

Dynamic wind loading is derived from wind time history and projected area [39], as shown in (10).

$$F_d(t) = 0.5\rho V(t)^2 C_d A_P \tag{10}$$

Air density, ρ, is chosen as 1.195kg/m^3. $V(t)$ is the wind time history, which is the sum of the mean wind and fluctuating wind components. Drag coefficient, C_d, is usually determined by the wind tunnel test [39]. In this research, we assume all wind loads are added on the transmission tower perpendicularly; thus, we choose the drag coefficient based on the literature with similar transmission tower shape and height [38], [39]. By adding wind load on the finite element model and simplified lumped mass model, the top tip displacement of transmission tower is demonstrated in Fig. 3.

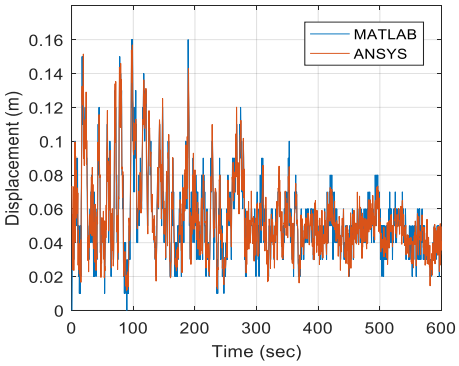

Fig. 3. The comparison of the top displacement between finite element and lumped mass models.

A. Transmission Tower Fragility under Extreme Wind

A fragility curve describes the likelihood of damage and failure of a structure under different loading intensity (earthquake ground motion intensity [40], wind speed, etc.). In structural wind fragility, the damage and failure probability $F_R(V)$ under a given wind speed Vcan be calculated as shown in (11).

$$F_R(V) = P[l > LS \mid V_{10} = V] \tag{11}$$

The damage condition is defined as the structure performance exceeding a limit state (LS). In this paper, the limit states are determined as transmission tower's top displacement over tower height is at 1.5%, 2%, 2.5% and 3%. Different fragility curves under different limit states are demonstrated in Fig. 4. The marked points are the probability of damage or failure of the individual tower under different wind speeds. The solid curve is the fitted normal cumulative distribution function. In this paper, the failure condition of all transmission towers is determined at a displacement of over 2.5%.

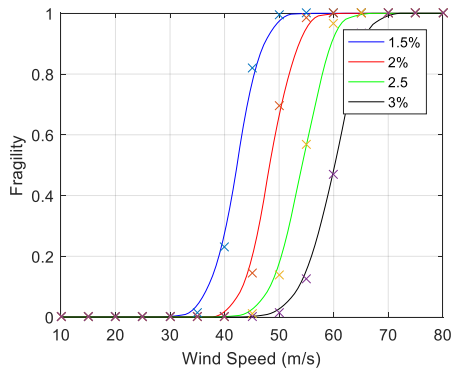

Fig. 4. Wind fragility curve of a transmission tower.

B. Transmission System Fragility under Extreme Wind

In order to estimate the performance of the transmission system in the hurricane region, two steps of calculation are involved. First, a horizontal wind profile is required to model the wind speed distribution in the region, affected by the hurricane. The horizontal wind profile can be express via (12) [41].

$$V_g(r_g) = \left[\frac{AB(p_n-p_c)\,exp\left(-\frac{A}{r_g{}^B}\right)}{\rho r_g{}^B} + \frac{r_g{}^2 f_c{}^2}{4}\right]^{1/2} - r_g f_c/2 \tag{12}$$

$V_g(r_g)$ is the gradient wind speed as a function of radial distance, r_g, from the hurricane center. This paper simplifies the

calculation of the gradient as only a function of the radius distance. Wind speed increases linearly when it is in the 100-km range of the hurricane center. Outside that range, wind speed shows a parabolic attenuation.

The second step to estimate the transmission system health condition requires a calculation of each transmission line's failure probability based on the m^{th} individual transmission tower's failure probability $P_m = F_{R,m}(V_m)$. We denote the k^{th} transmission line's failure probability by $P[FL,k]$, and its survival probability by $P[SL,k]$. For a transmission line to survive a wind load, all of its towers must survive. Thus, $P[FL,k]$ can be calculated as shown in (13).

$$P[FL,k] = 1 - P[SL,k] = 1 - \prod_{m=1}^{NT} F_{R,m}(V_m) \quad (13)$$

According to the horizontal wind profile and hurricane movement track, wind speed at each tower location at each time interval can be estimated. This paper assumes that the angle of wind is 0, as different wind directions occur on lower spatial scales rather than a specific angle [41].

IV. Transmission Outage Scenario Generation

Based on the likelihood of each transmission line to fail, transmission contingency scenarios can be generated and their probabilities can be also calculated. Since different lines may fail at different time during the hurricane, each scenario should indicate the lines that fail and the time when each of those lines go out of service. The scenario generation procedure is illustrated in Fig. 5.

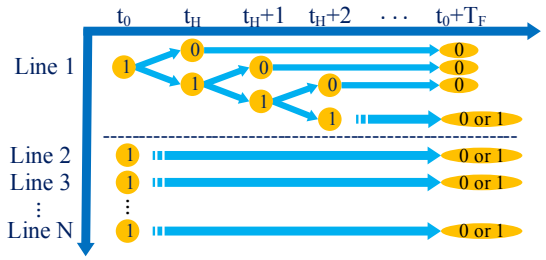

Fig. 5. Illustration of the scenario generation procedure.

According to Fig. 5, each scenario can be uniquely identified by a vector with N_{br} components, each of which indicating the time of failure for a particular line. If a line does not fail in a given scenario, the respective value for the line in the scenario vector should be greater than the time range of the study, i.e. $t_0 + T_F + 1$, which means that the line does not fail within the duration of the SCUC. The total number of scenarios can, thus, calculated as shown in (14).

$$N_s = (T_F + 1)^{N_{br}} \quad (14)$$

Given that transmission line k fails at t_k in scenario s, the probability for each scenario is calculated in (15).

$$p_s = \prod_{k=1}^{N_{br}} \left(p_{k,t_k} \prod_{t=t_H}^{t_k-1} (1 - p_{k,t})\right) \quad (15)$$

(14) clearly shows how the number of scenarios can grow very quickly as the number of lines that are affected increases. The size of the scenario set greatly impacts the computational time, required for solving the optimization problem. Thus, it is essential to reduce the scenario size to an acceptable level. In this paper, we use a very simple method and filter out the scenarios that have a probability below a cutoff level.

V. Preventive Stochastic Optimization Model

The proposed preventive stochastic optimization model is based on a DC unit commitment (UC) formulation. The formulation explicitly models the transmission outage scenarios, caused by the hurricane. The problem identifies a single unit commitment solution for all the scenarios, while allowing generation dispatch to vary under each scenario, as long as the ramping limits are not violated. Both over-generation and load shedding are allowed under the scenarios, but penalized with a high penalty price in the objective function.

The formulation of the problem is shown in (16) – (28). The objective function is expressed in (16), which minimizes the expected dispatch cost of the system considering generation dispatch, over-generation and load shedding under all scenarios. Generation limits are expressed in (17) – (19); generation costs were calculated using a piece-wise linear cost function. DC power flow constraints are expressed in (20) and (21); when a transmission line is out of service, both its susceptance and capacity limit are set to 0 using the binary integer parameter $z_{k,s,t}$. (22) sets the voltage angle of the reference bus to 0. (23) is the nodal power balance constraint in which over-generation and load shedding are included. (24) and (25) calculate the start-up and shut-down variables; (26) is the hourly ramping limit for each generator; (27) and (28) are the minimum up and down time constraints for each generator. Since the contingencies are explicitly modeled, reserve requirements are omitted.

$$\min \left(\sum_{s=1}^{N_s} p_s \sum_{t=1}^{T} \left(\sum_{g=1}^{N_g} \left(\sum_{seg=1}^{N_{seg}} c_{g,seg}^{linear} P_{g,s,t}^{seg} + c_g^{NL} u_{g,t} + c_g^{SU} v_{g,t} + c_g^{SD} w_{g,t} + c^O P_{g,s,t}^O \right) + \sum_{n=1}^{N_b} c^L L_{n,s,t}^L \right) \right) \quad (16)$$

$$P_{g,s,t} = \sum_{seg=1}^{N_{seg}} P_{g,s,t}^{seg} \quad (17)$$

$$0 \le P_{g,s,t}^{seg} \le P_g^{seg,max} \quad (18)$$

$$u_{g,t} P_g^{min} \le P_{g,s,t} \le u_{g,t} P_g^{max} \quad (19)$$

$$-z_{k,s,t} F_k^{max} \le F_{k,s,t} \le z_{k,s,t} F_k^{max} \quad (20)$$

$$z_{k,s,t} b_k \left(\theta_{fr,k,s,t} - \theta_{to,k,s,t}\right) = F_{k,s,t} \quad (21)$$

$$\theta_{1,s,t} = 0 \quad (22)$$

$$\sum_{k \in \sigma^+(n)} F_{k,s,t} - \sum_{k \in \sigma^-(n)} F_{k,s,t} + \sum_{g \in g(n)} P_{g,s,t} - P_{g,s,t}^O = L_{n,s.t} - L_{n,s,t}^L \quad (23)$$

$$v_{g,t} - w_{g,t} = u_{g,t} - u_{g,t-1} \quad (24)$$

$$v_{g,t} + w_{g,t} \le 1 \quad (25)$$

$$-RR_g \le P_{g,s,t} - P_{g,s,t-1} \le RR_g \quad (26)$$

$$\sum_{t=m}^{m+T_g^{up}-1} u_{g,t} \ge T_g^{up} \left(u_{g,m} - u_{g,m-1}\right), \quad 2 \le m \le T - T_g^{up} + 1 \quad (27)$$

$$\sum_{t=m}^{m+T_g^{down}-1} (1 - u_{g,t}) \ge T_g^{down} \left(u_{g,m-1} - u_{g,m}\right), \quad 2 \le m \le T - T_g^{down} + 1 \quad (28)$$

VI. Simulation Studies

This section studies the effectiveness of the developed model through simulation on the IEEE 118-bus system [42]. To provide a better understanding, two separate cases are built, where

the hurricanes affect different parts of the system. First, we mapped the IEEE 118-bus system to the transmission network in Texas. The first case chooses 13 buses from IEEE 118-bus and 19 transmission lines as shown in in Fig. 6-left, denoted as layout I. The second case chooses 20 buses and 23 lines as shown in Fig. 6-right, denoted as layout II. Two hurricane scenarios were also generated, imitating Hurricane Harvey and Irma. As the primary objective of this paper is to explore the feasibility and effectiveness of preventive operation, incorporating weather information, the simulation studies assume that the weather forecast is exact. In both scenarios, the maximum sustained wind speed is extracted from the National Hurricane Center database [43]. Fig. 7-top shows Hurricane Harvey's peak wind speed from 4 am August 26th to 4 am August 27th and Fig. 7-bottom shows Hurricane Irma's peak wind speed from 5 pm September 9th to 5 pm September 10th. According to section III, horizontal wind speed profile can be approximated as shown in Fig. 8.

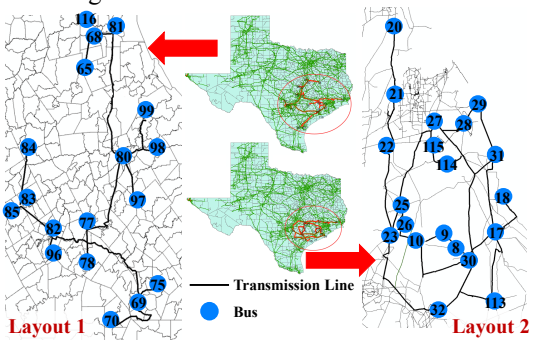

Fig. 6. Two mappings of IEEE 118-bus system on Texas transmission grid.

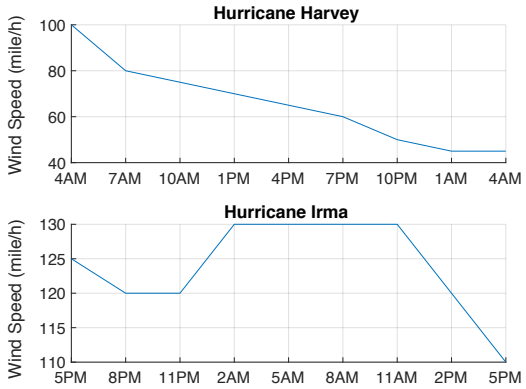

Fig. 7. Peak wind speed of Hurricane Harvey and Irma for 24 hours

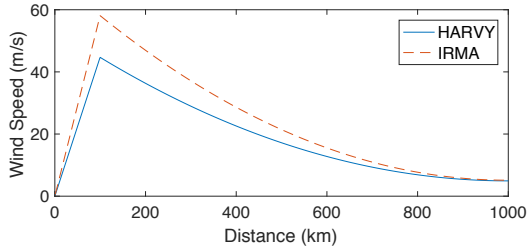

Fig. 8. Horizontal wind profile as a function of radius distance.

A. Transmission System Fragility Analysis

According to the transmission system analysis procedure, described in Section III, failure probabilities of the transmission lines under Hurricane Harvey and Irma equivalent scenarios can be estimated. Such accumulated probabilities at different time intervals are provided in TABLE I-TABLE III.

TABLE I
TRANSMISSION LINE FAILURE PROBABILITIES UNDER HARVEY

Harvey I			**Harvey II**		
Line number	4AM	7AM – 4AM	Line number	4AM	7AM-4AM
69-70	0	0	10-9	0.95	0.95
69-75	0	0	9-8	0.96	0.96
69-77	0	0	8-30	0.49	0.49
78-77	0	0	30-17	0.74	0.74
82-77	0	0	17-18	0.96	0.96
82-96	0	0	17-113	0.55	0.55
82-83	0	0	113-32	0	0
85-83	0	0	32-31	0.96	0.96
84-83	0	0	29-31	0.99	0.99
77-80	0.63	0.63	28-29	0.99	0.99
97-80	0.83	0.83	27-28	0.99	0.99
98-80	0.96	0.96	27-115	0.99	0.99
99-80	0.99	0.99	114-115	0.99	0.99
80-79	0.96	0.96	114-32	0.98	0.98
80-81	0.99	0.99	27-32	0.99	0.99
65-68	0.95	0.95	27-25	1	1
68-116	0.99	0.99	26-25	0.60	0.60
66-65	0.16	0.15	23-25	0.42	0.42
69-68	0.93	0.93	23-32	0.14	0.14
			23-22	0.88	0.88
			21-22	0.94	0.94
			20-21	0.89	0.89
			26-30	0.51	0.51

TABLE II
TRANSMISSION LINE FAILURE PROBABILITIES UNDER IRMA I

Line number	**5PM**	**8PM**	**11PM**	**2AM**	**5AM**	**8AM -5PM**
69-70	0	0	0	0.99	1	1
69-75	0	0	0.33	1	1	1
69-77	0.01	0.86	1	1	1	1
78-77	0	0.42	1	1	1	1
82-77	0	0.65	1	1	1	1
82-96	0	0.01	0.98	1	1	1
82-83	0	0.20	1	1	1	1
85-83	0	0.01	0.91	1	1	1
84-83	0.09	0.55	1	1	1	1
77-80	1	1	1	1	1	1
97-80	1	1	1	1	1	1
98-80	1	1	1	1	1	1
99-80	1	1	1	1	1	1
80-79	1	1	1	1	1	1
80-81	1	1	1	1	1	1
65-68	1	1	1	1	1	1
68-116	1	1	1	1	1	1
66-65	0.78	1	1	1	1	1
69-68	1	1	1	1	1	1

TABLE III
TRANSMISSION LINE FAILURE PROBABILITIES UNDER IRMA II

Line number	**5PM**	**8PM**	**11PM-5PM**
10-9	1	1	1
9-8	1	1	1
8-30	1	1	1
30-17	1	1	1
17-18	1	1	1
17-113	1	1	1
113-32	0.11	1	1
32-31	1	1	1
29-31	1	1	1
28-29	1	1	1
27-28	1	1	1
27-115	1	1	1
114-115	1	1	1
114-32	1	1	1
27-32	1	1	1
27-25	1	1	1
26-25	1	1	1
23-25	1	1	1
23-32	1	1	1
23-22	1	1	1
21-22	1	1	1
20-21	1	1	1
26-30	1	1	1

B. Transmission Outage Scenarios

Using the information provided in the TABLE I-TABLE III, all the possible transmission outage scenarios were generated for the four cases (two hurricanes passing through two different parts of the system). Each scenario is a vector, including information about the status of all the transmission lines at each hour in the studied period. In order to reduce computational burden, scenarios with a probability of less than 0.1% were eliminated. The probabilities of the remaining scenarios were adjusted proportionally, so that they sum up to 1. The number of simulated scenarios for each case is shown in TABLE IV.

TABLE IV
NUMBER OF SCENARIOS CONSIDERED IN EACH CASE

Hurricane cases	Harvey I	Harvey II	Irma I	Irma II
Number of scenarios	40	157	134	2

C. Preventive Operation

Hurricane Harvey made landfall around 4:00 am, and it was able to cause transmission line failures only in the first three hours, so the uncertainty of transmission line failures caused by this hurricane exists only on the day that the hurricane made its landfall. However, for the case of Hurricane Irma, it made its landfall around 5:00 pm, and was able to cause transmission line failures over the next 15 hours. Thus, the uncertainty of damage lasts into two days. In order to study the impact of the two hurricanes in a sufficiently long period, while considering the industrial practices for operating a day-ahead market, the impact of Hurricane Harvey was studied in a 24-hour UC model, while that of Hurricane Irma was studied in a 48-hour UC model. The simulations were carried out in the following manner: 1. Two deterministic unit commitment models, without considering the outage scenarios, were carried out as base cases according to the base case formulation presented in [44], one over 24 hours and the other over 48 hours. 2. The unit commitment results were obtained from the two base cases and fixed in the stochastic model, to calculate the expected load shedding and over-generation under the hurricane scenarios with business as usual (BAU) operation. 3. The UC was optimized using the stochastic model, in order to evaluate the impact of the hurricanes with the preventive UC model. Steps 2 and 3 were carried out for the four cases listed in TABLE IV. As both load shedding and over-generation are undesirable, they were penalized with a penalty factor of $10,000/MWh in the stochastic model.

The expected dispatch costs were obtained for the four cases under both BAU and the proposed preventive model, and compared with the base cases in TABLE V. The results are presented both including and excluding the penalties for over-generation and load shedding. As the penalty price is very large, the cost is dominated by its penalty component, when penalties are included. In such cases, the preventive model shows an obvious advantage in terms of achieving a lower cost solution, as it effectively reduces over-generation and load shedding. It is difficult to compare the costs, when penalties are excluded, because the cost will generally decrease as more load is shed. Thus, comparison purely based on cost is not very meaningful here. However, in 3 out of 4 cases, the stochastic preventive model converges to a higher cost solution both compared to the base case and BAU. The largest increase from the base case is for Harvey II, where the preventive model adds 51% to the cost. However, the additional cost will help significantly enhance the system reliability as will be discussed later in TABLE VI.

TABLE V
EXPECTED COST COMPARISON ($M)

Hurricane case	Base case	BAU w/ penalties	Preventive model w/ penalties	BAU w/o penalties	Preventive model w/o penalties
Harvey I	1.14	57.09	33.97	1.01	1.11
Harvey II	(1 day)	160.48	32.96	1.15	1.72
Irma I	2.28	154.49	105.49	2.00	2.33
Irma II	(2 days)	388.35	66.83	2.17	3.10

The expected load shedding and over-generation from the four cases, under BAU and preventive operation, were calculated as a percentage of the overall demand during the studied period and presented in TABLE VI. In all cases, the preventive model was able to reduce the violations anywhere between 33% and 83%. As the damages for layout II was especially significant, with the BAU model, not only did the load shedding double, but also there was a 4-7% of over-generation, which caused much larger penalty costs compared to layout I. Using the preventive UC model, over-generation was practically eliminated, and the expected load shedding was reduced to much lower levels, even for the case of Irma II, with a stronger hurricane and a more vulnerable layout. Thus, the mediocre increase in costs, presented in TABLE V, is essentially the cost of reliability enhancement, which is rather significant, as shown in TABLE VI.

TABLE VI
EXPECTED LOST LOAD AND OVER GENERATION

Hurricane case	BAU		Preventive operation	
	Expected lost load	Expected over-generation	Expected lost load	Expected over-generation
Harvey I	6.23%	0.00%	3.65%	0.00%
Harvey II	12.91%	4.79%	3.46%	0.01%
Irma I	8.47%	0.00%	5.73%	0.00%
Irma II	15.25%	6.20%	3.54%	0.00%

VII. COMPUTATIONAL COMPLEXITY

The optimization problem, developed in this paper, is a stochastic mixed-integer linear program. Solution time in this class of problems is heavily influenced by the number of integer variables and scenarios. The solution times for the four cases, presented in this paper, are shown in TABLE VII. For instance, Harvey II and Irma I had similar number of scenarios, but Irma I was solved over 48 hours, while Harvey II was solved over 24 hours. Thus, Irma I involved a larger number of variables, especially binary commitment variables. This made the solution time for Irma I significantly longer than Harvey II. Harvey I and Irma II had relatively small numbers of scenarios, and both of them were solved in a relatively short period of time. It should be noted that the solution time can be substantially longer for larger systems. Thus, alternative formulations and more rigorous scenario reduction techniques should be implemented to further reduce the solution time.

TABLE VII
SOLUTION TIME OF THE FOUR CASES

Hurricane case	Harvey I	Harvey II	Irma I	Irma II
Solution time (min)	46.63	494.51	2889.28	0.31

VIII. Conclusions

This paper, for the first time, develops an integrated model, where weather forecast information is effectively incorporated in power system operation. First, a finite element structural model of the transmission towers is developed. The model takes weather data as an input and calculates the failure probability of the transmission lines. These probabilities are, then, explicitly included within a day-ahead unit commitment model. Thus, the integrated framework is able to guide effective preventive operation under extreme weather conditions. The proposed model was validated against business as usual operation under Hurricane Irma and Harvey, synthesized for IEEE 118-bus system. To explore the feasibility and effectiveness of preventive operation, incorporating weather information, the simulation studies assumed that the weather forecast is exact. The results suggest that the proposed integrated model is able to drastically reduce power outages (33%-83%), during hurricanes by moderately increasing the operation cost (up to 51%). Further research is required for improving the computational efficiency of the developed model and testing on real-world large-scale systems. Future research will also study the impacts of weather forecast uncertainty on effectiveness of preventive operation.

IX. References

[1] The President's Council of Economic Advisers and DOE, "Economic Benefits of Increasing Electric Grid Resilience to Weather Outages," White House Office of Science and Technology, U.S. DOE, Aug. 2013.

[2] P. Hines, J. Apt, and S. Talukdar, "Large blackouts in North America: Historical trends and policy implications," *Energy Policy*, vol. 37, no. 12, pp. 5249–5259, 2009.

[3] Argonne National Laboratory, *National Electricity Emergency Response Capabilities*. U.S. Department of Energy.

[4] U.S. Department of Energy, Infrastructure Security and Energy Restoration, *Hurricane Harvey Event Report (Update 4)*.

[5] U.S. Department of Energy, Infrastructure Security and Energy Restoration, *Hurricane Irma and Hurricane Harvey Event Summary (Report 26)*.

[6] U.S. Department of Energy, Infrastructure Security and Energy Restoration, *Hurricane Irma and Hurricane Harvey Event Summary (Report 28)*.

[7] U.S. Department of Energy, Infrastructure Security and Energy Restoration, *Hurricanes Maria, Irma, and Harvey September 22 Afternoon Event Summary (Report 43)*.

[8] A. Lisnianski, G. Levitin, H. Ben-Haim, and D. Elmakis, "Power system structure optimization subject to reliability constraints," *Electr. Power Syst. Res.*, vol. 39, no. 2, pp. 145–152, 1996.

[9] G. Levitin, A. Lisnianski, and D. Elmakis, "Structure optimization of power system with different redundant elements," *Electr. Power Syst. Res.*, vol. 43, no. 1, pp. 19–27, 1997.

[10] Z. Xie, G. Manimaran, V. Vittal, A. Phadke, and V. Centeno, "An information architecture for future power systems and its reliability analysis," *IEEE Trans. Power Syst.*, vol. 17, no. 3, pp. 857–863, 2002.

[11] North American Electric Reliability Corporation (NERC), *Criteria for Reliability Coordinator Actions to Operate Within IROLs - NERC Standard IRO-008-1*. NERC, 2014.

[12] North American Electric Reliability Corporation (NERC), *Criteria for Reliability Coordinator Actions to Operate Within IROLs - NERC Standard IRO-009-1*. NERC, 2014.

[13] Testimony of Walt Baum—Executive Director Texas Public Power Association, *Resiliency: The Electric Grid's Only Hope*. House Science, Space, and Technology Committee, 2017.

[14] North American Electric Reliability Corporation (NERC), *Hurricane Sandy Event Analysis Report*. NERC, 2014.

[15] K. Zhou, C. Fu, and S. Yang, "Big data driven smart energy management: From big data to big insights," *Renew. Sustain. Energy Rev.*, vol. 56, pp. 215–225, 2016.

[16] D. Zhu, D. Cheng, R. P. Broadwater, and C. Scirbona, "Storm modeling for prediction of power distribution system outages," *Electr. Power Syst. Res.*, vol. 77, no. 8, pp. 973–979, 2007.

[17] R. Nateghi, S. Guikema, and S. M. Quiring, "Power outage estimation for tropical cyclones: Improved accuracy with simpler models," *Risk Anal.*, vol. 34, no. 6, pp. 1069–1078, 2014.

[18] H. Liu, R. A. Davidson, and T. V. Apanasovich, "Statistical forecasting of electric power restoration times in hurricanes and ice storms," *IEEE Trans. Power Syst.*, vol. 22, no. 4, pp. 2270–2279, 2007.

[19] S. R. Han, *Estimating hurricane outage and damage risk in power distribution systems*. Texas A&M University, 2008.

[20] S. D. Guikema, S. M. Quiring, and S.-R. Han, "Prestorm estimation of hurricane damage to electric power distribution systems," *Risk Anal.*, vol. 30, no. 12, pp. 1744–1752, 2010.

[21] J. Winkler, L. Duenas-Osorio, R. Stein, and D. Subramanian, "Performance assessment of topologically diverse power systems subjected to hurricane events," *Reliab. Eng. Syst. Saf.*, vol. 95, no. 4, pp. 323–336, 2010.

[22] S. D. Guikema, R. Nateghi, S. M. Quiring, A. Staid, A. C. Reilly, and M. Gao, "Predicting hurricane power outages to support storm response planning," *IEEE Access*, vol. 2, pp. 1364–1373, 2014.

[23] Y. Wang, C. Chen, J. Wang, and R. Baldick, "Research on resilience of power systems under natural disasters—A review," *IEEE Trans. Power Syst.*, vol. 31, no. 2, pp. 1604–1613, 2016.

[24] A. Arab, A. Khodaei, Z. Han, and S. K. Khator, "Proactive recovery of electric power assets for resiliency enhancement," *IEEE Access*, vol. 3, pp. 99–109, 2015.

[25] A. Arab, A. Khodaei, S. K. Khator, K. Ding, V. A. Emesih, and Z. Han, "Stochastic pre-hurricane restoration planning for electric power systems infrastructure," *IEEE Trans. Smart Grid*, vol. 6, no. 2, pp. 1046–1054, 2015.

[26] P. Van Hentenryck and C. Coffrin, "Transmission system repair and restoration," *Math. Program.*, vol. 151, no. 1, pp. 347–373, 2015.

[27] C. Coffrin and P. Van Hentenryck, "Transmission system restoration with co-optimization of repairs, load pickups, and generation dispatch," *Int. J. Electr. Power Energy Syst.*, vol. 72, pp. 144–154, 2015.

[28] C. Wang, Y. Hou, F. Qiu, S. Lei, and K. Liu, "Resilience Enhancement With Sequentially Proactive Operation Strategies," *IEEE Trans. Power Syst.*, vol. 32, no. 4, pp. 2847–2857, 2017.

[29] M. Sahraei-Ardakani and G. Ou, "Day-Ahead Preventive Scheduling of Power Systems During Natuaral Hazards via Stochastic Optimization," in *IEEE PES General Meeting*, Chicago, IL, 2017, pp. 1–5.

[30] P. A. Hirschberg *et al.*, "A Weather and Climate Enterprise Strategic Implementation Plan for Generating and Communicating Forecast Uncertainty Information," *Bull. Am. Meteorol. Soc.*, vol. 92, no. 12, pp. 1651–1666, Aug. 2011.

[31] P. Hoffman, W. Bryan, and A. Lippert, "Comparing the Impacts of the 2005 and 2008 Hurricanes on US Energy Infrastructure," *US Dep. Energy*, 2009.

[32] B. Asgarian, S. Dadras Eslamlou, A. E. Zaghi, and M. Mehr, "Progressive collapse analysis of power transmission towers," *J. Constr. Steel Res.*, vol. 123, no. Supplement C, pp. 31–40, Aug. 2016.

[33] B. Chen, W. Guo, P. Li, and W. Xie, "Dynamic Responses and Vibration Control of the Transmission Tower-Line System: A State-of-the-Art Review," *The Scientific World Journal*, 2014.

[34] H. Yasui, H. Marukawa, Y. Momomura, and T. Ohkuma, "Analytical study on wind-induced vibration of power transmission towers," *J. Wind Eng. Ind. Aerodyn.*, vol. 83, no. 1, pp. 431–441, 1999.

[35] J. D. Holmes, *Wind Loading of Structures, Third Edition*. CRC Press, 2015.

[36] G. Feng-lin, Y. Zhen-wei, D. Xiao-guang, and L. Xiao-lei, *Analysis of wind vibration in time domain of special high-voltage ±800kV Yangtze River long span transmission tower*. .

[37] A. G. Davenport, "The spectrum of horizontal gustiness near the ground in high winds," *Q. J. R. Meteorol. Soc.*, vol. 87, no. 372, pp. 194–211, 1961.

[38] M. Shinozuka and C.-M. Jan, "Digital simulation of random processes and its applications," *J. Sound Vib.*, vol. 25, no. 1, pp. 111–128, Nov. 1972.

[39] T. Mara, "Capacity Assessment of a Transmission Tower under Wind Loading," *Electron. Thesis Diss. Repos.*, Aug. 2013.

[40] B. R. Ellingwood, "Earthquake risk assessment of building structures," *Reliab. Eng. Syst. Saf.*, vol. 74, no. 3, pp. 251–262, 2001.

[41] G. J. Holland, "An analytic model of the wind and pressure profiles in hurricanes," *Mon. Weather Rev.*, vol. 108, no. 8, pp. 1212–1218, 1980.

[42] University of Washington, *Power Systems Test Case Archive: IEEE 118-Bus Test System*.

[43] N. H. Center, "National Hurricane Center." [Online]. Available: http://www.nhc.noaa.gov/. [Accessed: 04-Jan-2018].

[44] Y. Sang and M. Sahraei-Ardakani, "The Interdependence between Transmission Switching and Variable-Impedance Series FACTS Devices," *IEEE Trans. Power Syst.*, 2017.